Supporting Information

Lipinski et al. 10.1073/pnas.1009485107

SI Materials and Methods

Cell Lines and Culture Conditions. H4 human neuroblastoma cells were cultured under standard TC conditions in DMEM media supplemented with 10% normal calf serum, 1× penicillin/streptomycin, and 1× Na pyruvate (Invitrogen). GFP-LC3, FYVE-dsRed, GFP-LC3 pSRP-Beclin1 knock-down (1, 2) and Lamp-1-RFP (3) H4 cells have been previously described.

For antioxidant assay cells were treated 24 h after plating or siRNA transfection with NAC (Sigma) at 2.5 mM and cultured for an additional 6–48 h.

Amyloid β (Aβ) was prepared using a modified method from ref. 4. Briefly, the $A\beta_{1-40}$ peptide (Bachem) was dissolved in H_20, diluted 1:1 with 2× buffer (0.2 M Tris·HCl, pH 7.4, + 0.04% (wt/vol) sodium azide) and incubated at 37 °C for 24–72 h. Cells were treated 24 h after plating or siRNA transfection at 5-μM final concentration for 6–48 h.

For western blot analysis, lysosomal protease inhibitor E64d (Sigma) was added at 10 μg/mL unless otherwise indicated for the last 8–24 h before cell lysis.

siRNA Transfection. The genome-wide screen to identify genes regulating and mediating autophagy has previously been described (3). Briefly, for the Bcl2 and NAC high-throughput assays, we used an arrayed library of siRNAs (autophagy hits from the screen of Dharmacon si*ARRAY* siRNA library (Human Genome, G-005000–05, Thermo Fisher Scientific), with each gene covered by four independent oligonucleotides. Each assay plate included 10–12 wells of nontargeting siRNA as well as mTOR, ATG5, PLK1, and, depending on screen, Vps34 or SOD1 siRNA controls. siRNAs were transiently transfected at 30 nM final concentration in duplicate or triplicate into H4 GFP-LC3, FYVE-dsRed, Bec1+GFP-LC3, or Bec1+FYVE-dsRed cells, as indicated, using reverse transfection with HiPerfect reagent (Qiagen). Cells were incubated for 72 h under standard culture conditions; where indicated, NAC was added at at 2.5 mM after the first 24 h in culture. Cells were fixed by the addition of 30 μL 8% paraformaldehyde, counterstained with 0.5 μM Hoechst 33342 (Invitrogen), and washed three times with PBS.

For low-throughput follow-up assays, cells were transfected in 12- or six-well plates using reverse transfection with 1–6 μL HiPerfect/mL, 10–30 nM final siRNA concentration, and cells at 2.5×10^4 to 1×10^5 cells/mL. For western and imaging analysis, cells were split 24 h after transfection into 24-, 96-, or 384-well plates at $2.5–5.0 \times 10^4$ cells/mL and harvested after an additional 24–48 h.

Imaging and Image Quantification. Cells were imaged as previously described (3) on an automated CellWoRx microscope (Applied Precision) at 10× magnification. All images were quantified using VHSscan and VHSview image analysis software (Cellomics). The final GFP-LC3 and FYVE-dsRed vesicular translocation score was obtained by multiplying total autophagosome intensity/cell times number of autophagosomes/cell and dividing by average cells intensity. In the case of Lamp-1-RFP, which measures total accumulation of the reporter rather than its translocation, division by the average cell intensity was omitted.

Statistical Analysis. The statistical analysis used for the screen was as previously described (3). Briefly, all data were normalized by conversion to logarithmic scale (log10). z-Scores were calculated based on nontargeting siRNA control mean and SD, with scores greater than 1.5 and less than −1.5 considered significant. Relative viability was calculated by dividing number of cells in each well based on Hoechst imaging by the average cell number in the plate.

Unless otherwise indicated, *P* values were calculated from a two-tailed Student *t* test with equal variance. Error bars represent SEM.

Western Analysis. Cells were lysed in Lammeli sample buffer, resolved on 10–12% SDS/PAGE, and transferred to PVDF membrane according to standard protocols. The following antibodies were used: LC3 (Novus), p62 (Pharmigen), Sod1 (Cell Signaling), and Bcl-2 (Santa Cruz), all at 1:1,000; phospho-S6 (Ser235/236) (Cell Signaling) at 1:2,000; and tubulin (Sigma) at 1:5,000. Where indicated, blots were quantified using National Institutes of Health ImageJ64 software.

Semiquantitative RT-PCR. Total RNA was prepared using RNeasy mini kit (Qiagen) according to the manufacturer's instructions. A 1.25-μg quantity of RNA was used for cDNA synthesis using SuperScript First-Strand Synthesis System for RT-PCR (Invitrogen) with oligo dT primers. cDNA was diluted to 100 μL final volume; 5 μL was used for PCR with following primers: Cox5a cctacgtgctccgcccgctgtga and cttatgaggtcctgctttgtcc; β-actin gacctgacagactacctcat and AGACAGCACTGTGTTGGCTA.

Quantitative Real-Time RT-PCR. Real-time quantitative RT-PCR was carried out on an iCycler iQ system (BioRad) using SYBR Green one step PCR/RT-PCR kits (Qiagen). All reactions were performed in a 25-μL mixture containing 1× SYBR reaction buffer, 0.5 μM primers (FGF2: agagcgaccctcacatcaag and actgcccagttcgtttcagt; FGFR1: gcctgtggaggaacttttca and tggacaggtccaggtactcc), 10 nM fluorescein calibration dye (Bio-Rad), and 1 ng total RNA. A standard curve derived from 10-fold serial dilutions of purified RT-PCR products of the target gene was used to determine absolute concentrations of target RNA. Fluorescence from incorporated SYBR Green was captured at the end of each cycle and continuously during the melting curves. The fluorescence threshold value was determined by the iCycle iQ system software, and was further converted into concentration according to the standard curve. For QRT-PCR, the concentration of a given gene was normalized to the β-actin internal control.

Quantification of Cellular ROS Levels. By imaging: ROS were quantified 72 h after siRNA transfection or at indicated timepoints following Aβ treatment using Image-iT LIVE Green ROS Detection Kit for microscopy (Molecular Probes) according to manufacturers instructions. Images were acquired immediately on a Nikon Eclipse E800 microscope at 40× magnification and quantified using CellProfiler software (5).

Bioinformatics Analysis. ***Gene set enrichment analysis (GSEA).*** Associations of autophagy gene sets with AD were evaluated using GSEA (6) and gene expression data from laser-capture microdissected non–tangle-bearing neurons of 34 clinically and neuropathologically classified late-onset AD-afflicted individuals with a mean age at death of 79.9 ± 6.9 y and 14 neurologically normal healthy elderly controls (7) (GEO Accession No. GSE5281). This dataset includes a total of 161 Affymetrix Human Genome U133 Plus 2.0 arrays on six distinct brain regions from cases and controls (entorhinal cortex, hippocampus, medial temporal gyrus, posterior cingulate, superior frontal gyrus, and primary visual cortex). Affymetrix .CEL files were normalized to "all probe sets" in

a standardized matter, and scaled to 100 by the MAS5 algorithm implemented in the Bioconductor package (8) as previously described (9). GSEA, a nonparametric pathway analysis method (6, 10), was then used to determine whether predefined gene set were enriched at the top or bottom of a list of all genes assayed rank-ordered by their association with the phenotype using signal-to-noise ratio. For each autophagy gene set, an enrichment score was calculated, which is a weighted Kolmogorov–Smirnov–like statistic (6, 10). To adjust for different sizes of gene sets, a positive (negative) normalized enrichment score (NES) was computed (6, 10). A phenotype-based random permutation procedure was than used to estimate the statistical significance of the NES. The nominal P value of the NES was calculated based on 1,000 permutations, and $P \leq 0.05$ was considered evidence of a significant enrichment.

Analysis of hit gene expression during aging. The analysis was based on Affymetrix HG-U133_Plus_2 microarray data of younger (≤40 y old) and older (≥70 y old) human brain samples (11). Array normalization, expression value calculation, and clustering analysis were performed using the dChip software (12) (www.dchip.org).

Gene ontology enrichment analysis. siRNA screen hit genes were classified into canonical pathways based of MSigDB (6). To assess the statistical enrichment or overrepresentation of these categories for the hit genes relative to their representation in the global set of genes examined in the siRNA screen, P values were computed using the hypergeometric probability distribution, which was implemented in the R language.

Protein interaction network. The network was constructed by iteratively connecting interacting proteins, with data extracted from genome-wide interactome screens (13, 14), from the databases HPRD (15), MINT (16), and REACTOME (17), and from curated literature entries. The network uses graph theoretic representations, which abstract components (gene products) as nodes and relationships (interactions) between components as edges, implemented in the Perl programming language.

1. Shibata M, et al. (2006) Regulation of intracellular accumulation of mutant Huntingtin by Beclin 1. *J Biol Chem* 281:14474–14485.
2. Zhang L, et al. (2007) Small molecule regulators of autophagy identified by an image-based high-throughput screen. *Proc Natl Acad Sci USA* 104:19023–19028.
3. Lipinski MM, et al. (2010) Multiple mTORC1 independent signaling pathways regulate autophagy through type III PI3 kinase under normal nutritional conditions. *Dev Cell* 18:1041–1052.
4. Walsh DM, et al. (1999) Amyloid beta-protein fibrillogenesis. Structure and biological activity of protofibrillar intermediates. *J Biol Chem* 274:25945–25952.
5. Carpenter AE, et al. (2006) CellProfiler: Image analysis software for identifying and quantifying cell phenotypes. *Genome Biol* 7:R100.
6. Subramanian A, et al. (2005) Gene set enrichment analysis: A knowledge-based approach for interpreting genome-wide expression profiles. *Proc Natl Acad Sci USA* 102:15545–15550.
7. Liang WS, et al. (2008) Altered neuronal gene expression in brain regions differentially affected by Alzheimer's disease: A reference data set. *Physiol Genom* 33:240–256.
8. Gentleman RC, et al. (2004) Bioconductor: Open software development for computational biology and bioinformatics. *Genome Biol* 5:R80.
9. Scherzer CR, et al. (2007) Molecular markers of early Parkinson's disease based on gene expression in blood. *Proc Natl Acad Sci USA* 104:955–960.
10. Subramanian A, Kuehn H, Gould J, Tamayo P, Mesirov JP (2007) GSEA-P: A desktop application for Gene Set Enrichment Analysis. *Bioinformatics* 23:3251–3253.
11. Loerch PM, et al. (2008) Evolution of the aging brain transcriptome and synaptic regulation. *PLoS One* 3:e3329.
12. Li C, Wong WH (2001) Model-based analysis of oligonucleotide arrays: Expression index computation and outlier detection. *Proc Natl Acad Sci USA* 98:31–36.
13. Ho Y, et al. (2002) Systematic identification of protein complexes in Saccharomyces cerevisiae by mass spectrometry. *Nature* 415:180–183.
14. Ito T, et al. (2001) A comprehensive two-hybrid analysis to explore the yeast protein interactome. *Proc Natl Acad Sci USA* 98:4569–4574.
15. Mishra GR, et al. (2006) Human protein reference database—2006 update. *Nucleic Acids Res* 34(Database issue):D411–D414.
16. Chatr-aryamontri A, et al. (2007) MINT: The Molecular INTeraction database. *Nucleic Acids Res* 35(Database issue):D572–D574.
17. Joshi-Tope G, et al. (2005) Reactome: A knowledgebase of biological pathways. *Nucleic Acids Res* 33(Database issue):D428–D432.

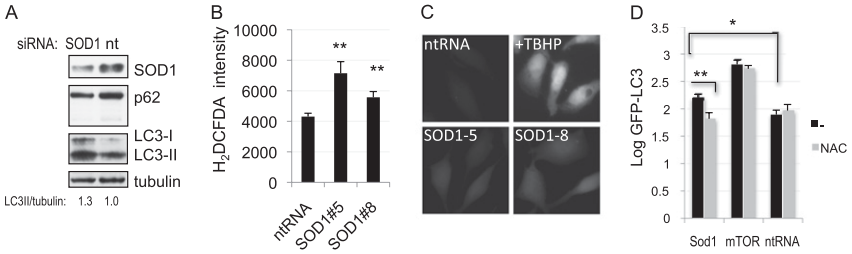

Fig. S1. Inactivation of SOD1 leads to induction of ROS-dependent autophagy. (*A*) Up-regulation of autophagy in H4 cells transfected with siRNA against SOD1 or nontargeting siRNA (nt) for 72 h. Knock-down of SOD1 and levels of autophagy were investigated using antibodies against SOD1 or p62 and LC3, respectively. (*B*) Induction of ROS in H4 cells transfected with two independent siRNAs against SOD1 or nontargeting siRNA for 72 h. Cells were stained in 25 mM carboxy-H2DCFDA and Hoechst and imaged immediately on a fluorescent microscope at ×40 magnification. (*C*) Representative images from *B*. As a control, where indicated, cells were treated with 100 mM tetr-butyl hydroperoxide (TBHP) to induce ROS. (*D*) Quantification of autophagy in H4 GFP-LC3 cells transfected with siRNA against SOD1 or nontargeting control siRNA (ntRNA) for 72 h. Where indicated, 2.5 mM NAC was added for the last 24 h before cells were fixed, counterstained with Hoechst, and imaged on a high-throughput fluorescent microscope at 10× magnification.

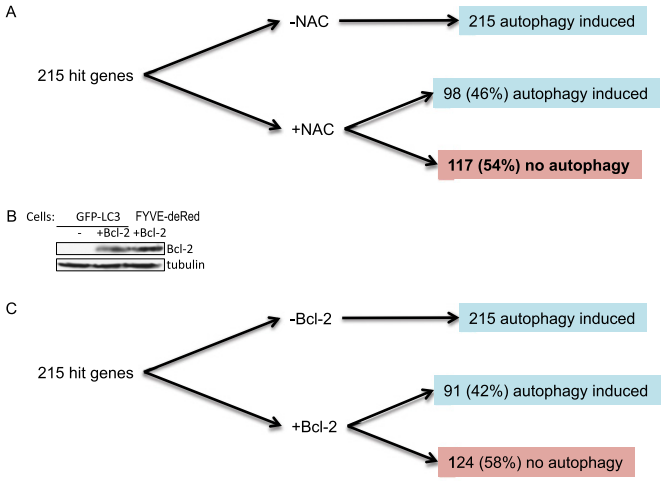

Fig. S2. Schematic representation of autophagy characterization screens for ROS and Bcl-2 dependence. (*A*) Induction of autophagy by 215 screen hits was compared in the absence or presence of antioxidant NAC in GFP-LC3 H4 cells. Cells were transfected with hit gene siRNAs or nontargeting control siRNA and cultured in the presence or absence of 2.5 mM NAC, as indicated, for 72 h, followed by fixation, counterstaining, and imaging at 10× on a high-throughput fluorescent microscope. (*B*) Bcl-2 expression in H4 GFP-LC3 and H4 FYVE-dsRed cells following infection with pBabe-Bcl-2 retrovirus and 1 mg/mL puromycin selection. (*C*) Induction of autophagy by 215 screen hits was compared in H4 cells stably expressing Bcl-2 or control cells. Cells were transfected and processed as in *A*.

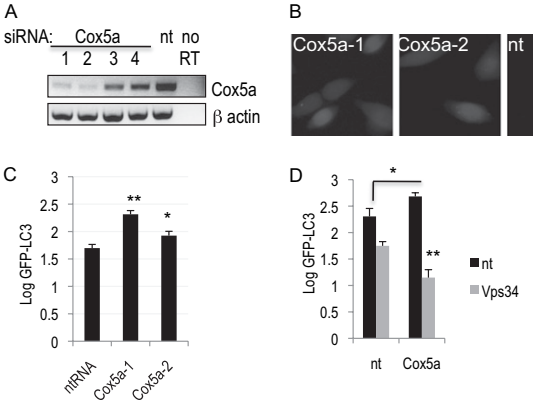

Fig. S3. Knock-down of the mitochondrial complex IV gene Cox5a leads to generation of ROS and induction of autophagy. (*A*) Confirmation of a knock-down of Cox5a. H4 cells were transfected with nontargeting control siRNA or siRNA against Cox5a for 72 h, followed by total RNA extraction and semiquantitative RT-PCR with primers against Cox5a or β actin. (*B*) Induction of ROS in H4 cells transfected with siRNAs against Cox5a or nontargeting siRNA for 72 h. Cells were stained in 25 mM carboxy-H2DCFDA and Hoechst and imaged immediately on a fluorescent microscope at 40× magnification. Representative images are shown. (*C*) Knock-down of Cox5a leads to the induction of autophagy. Cells were transfected with indicated siRNAs for 72 h; autophagy levels were by quantification of GFP-LC3 autophagosomal translocation. Cells were fixed, counterstained with Hoechst and imaged on a high-throughput fluorescent microscope at 10× magnification. (*D*) Induction of autophagy following Cox5a knock-down depends on the function of the type III PI3 kinase. Levels of autophagy induced following knock-down of Cox5a were assessed in H4 cells transfected with control nontargeting siRNA or siRNA against Vps34 for 72 h by Western blot. Cells were prepared and imaged as in *C*. $*P < 0.05$, $**P < 0.01$ based on two-tailed *t* test with equal variance. All error bars represent SEM.

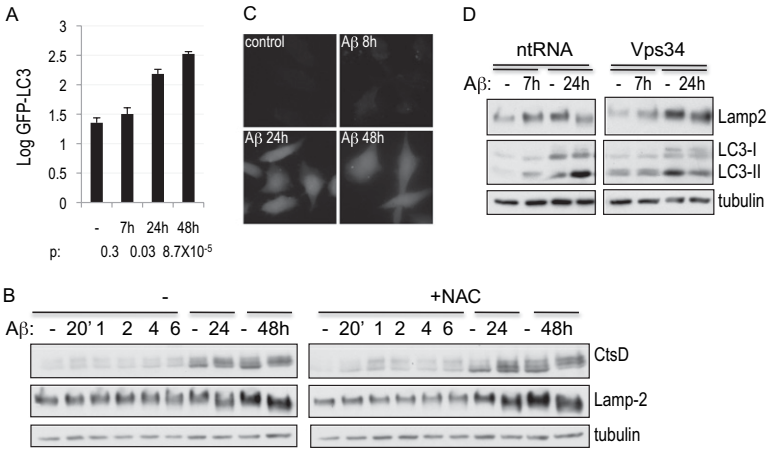

Fig. S4. Aβ up-regulates autophagy by inducing accumulation of ROS and the type III PI3 kinase activity. (*A*) Aβ induces autophagy. H4 GFP-LC3 cells were treated with 5 mM Aβ, followed by fixation, counterstaining, and high-throughput image acquisition at 10× magnification. (*B*) Aβ treatment leads to pathological changes in lysosomal proteins. H4 cells were treated as in *A;* lysosomal changes were investigated using antibodies against cathepsin D (CtsD) and Lamp 2. (*C*) Treatment with Aβ leads to the generation of ROS. Cells were treated with 5mM Aβ, stained in 25mM carboxy-H2DCFDA and Hoechst and imaged immediately on a fluorescent microscope at 40× magnification. Representative images are shown. (*D*) Induction of autophagy by Aβ is dependent on the type III PI3 kinase activity. H4 cells were transfected with siRNA against the type III PI3 kinase subunit Vps34 or nontargeting control siRNA and than treated as in *B*. Autophagy and lysosomal changes were investigated with antibodies against LC3 and Lamp 2, respectively. $^{**}P < 0.01$ based on two-tailed *t* test with equal variance. All error bars represent SEM.

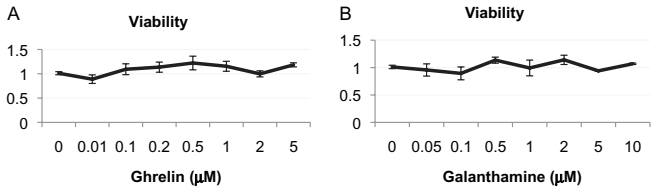

Fig. S5. Drugs against Alzheimer's disease suppress autophagy without compromising viability. H4 GFP-LC3 cells were treated with indicated concentrations of GSHR ligand Ghrelin (*A*) or CHRND agonist Galanthamine (*B*) for 24 h. Cells were fixed, counterstained, and imaged at 10× on a high-throughput fluorescent microscope. Viability was evaluated based on Hoechst counterstain. All error bars represent SEM.

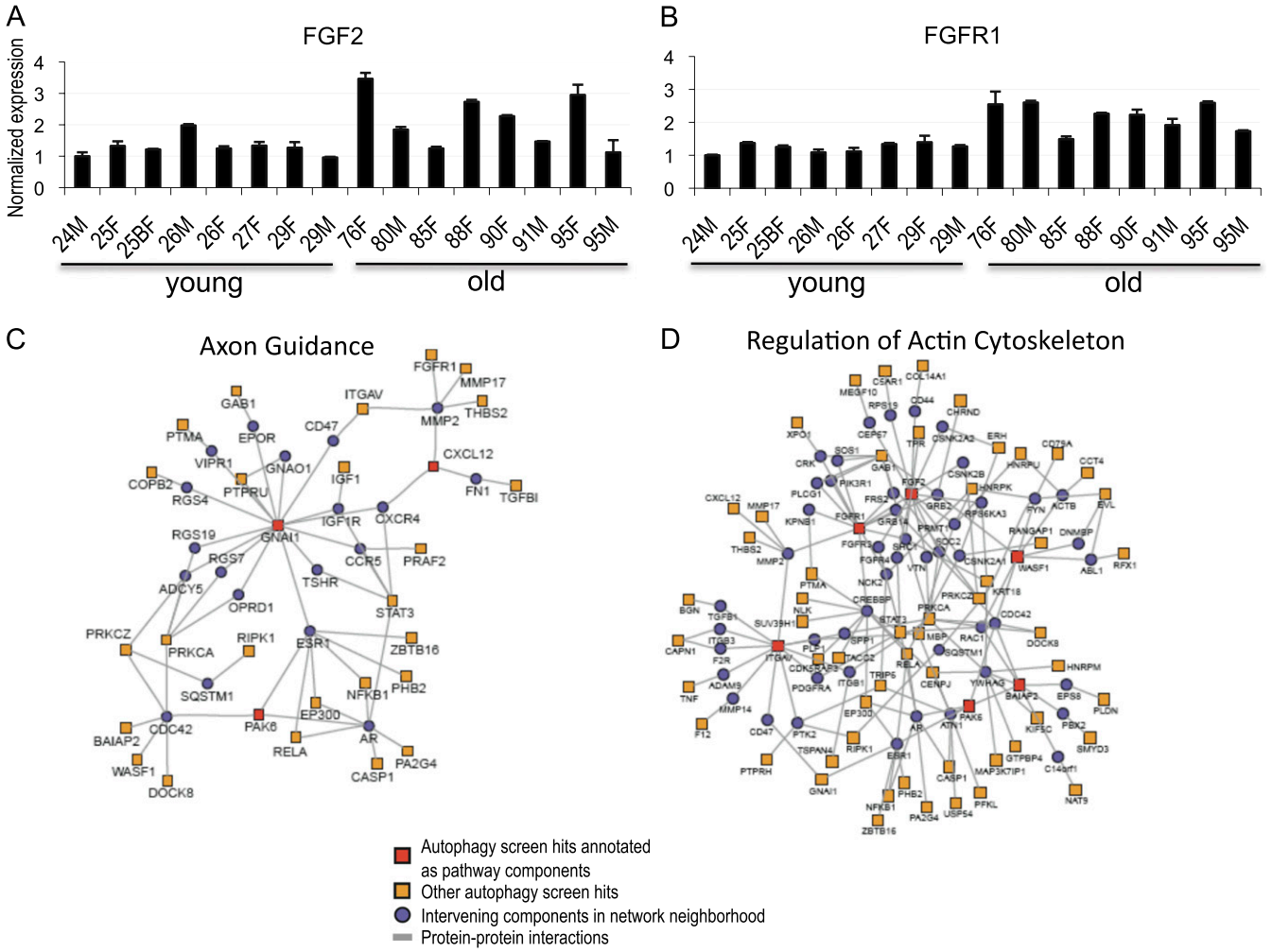

Fig. S6. Expression of autophagy genes during normal human aging and its importance for brain function. (*A* and *B*) Confirmation of microarray data for FGF2 and FGFR1 genes in younger (≤40 y old) versus older (≥70 y old) human brain samples by quantitative PCR. $P = 0.0281$ and $P = 0.0002$, respectively. (*C* and *D*) Network extensions of canonical pathways involved in the regulation of (*C*) axon guidance and (*D*) actin cytoskeleton. Using human interactome data, these pathway-centric networks were constructed by anchoring on canonical pathway components that scored in the screen, and extended by establishing connections with other hit genes by including at most one intervening component.

Other Supporting Information Files

Table S1 (XLS)
Table S2 (XLS)
Table S3 (XLS)
Table S4 (XLS)
Table S5 (XLS)
Table S6 (XLS)
Table S7 (XLS)
Table S8 (XLS)
Table S9 (XLS)